International Journal of Minerals, Metallurgy and Materials
Accepted manuscript, https://doi.org/10.1007/s12613-020-2076-2

Effects of CeO_2 pre-calcined at different temperatures on the performance of Pt/CeO_2-C electrocatalyst for MOR

Guo-qing Li[1‡)], Pu-kang Wen[1‡)], Chen-qiang Gao[2)], Tian-yi Zhang[2)], Jun-yang Hu[2)], Yu-hao Zhang[2)], Qing-feng Li[4)], Shi-you Guan[3*)] and Bing Li[1*)]

1) School of Mechanical and Power Engineering, East China University of Science and Technology, Shanghai 200237, China.

2) School of Materials Science and Engineering, East China University of Science and Technology, Shanghai 200237, China

3) Institute for Sustainable Energy, College of Sciences, Shanghai University, Shanghai 200237, China.

4) Department of Energy Conversion and Storage, Technical University of Denmark, Lyngby 2800, Denmark.

***Corresponding authors:** *Bing Li*[1*]

Mail Address: School of Mechanical and Power Engineering, East China University of Science and Technology, Shanghai 200237, China

Telephone: +86 13818307848

E-mail: drlibing@163.com , bingli@ecust.edu.cn (B. Li)

Shi-you Guan[3*]

Mail Address: Insitute for Sustainable Energy, College of Sciences, Shanghai University, Shanghai 200444, China

E-mail: syguan@shu.edu.cn (S. Guan)

‡ These authors contributed equally to this work.

Abstract

Pt/CeO_2-C catalysts with CeO_2 pre-calcined at 300~600°C were synthesized by combining hydrothermal calcination and wet impregnation method. The effects of the pre-calcined CeO_2 on the performance of Pt/CeO_2-C catalysts for methanol oxidation have been investigated. The Pt/CeO_2-C catalysts with pre-calcined CeO_2 at 300~600°C show an average particle size of 2.6-2.9 nm, and exhibit better methanol electro-oxidation catalysis activity than the commercial Pt/C catalyst. Specifically, the Pt/CeO_2-C catalysts with pre-calcined CeO_2 at 400°C display the highest electrochemical surface area (*ECSA*) value at 68.14 $m^2\ g^{-1}_{Pt}$ and I_f/I_b ratio at 1.26, which are far larger than that of the commercial Pt/C catalyst at 53.23 $m^2\ g^{-1}_{Pt}$ and 0.79 respectively, implying the greatly enhanced CO tolerance performance.

Key words: DMFC, Pt/CeO_2-C, Electrocatalysts, Methanol oxidation

1. Introduction

Direct methanol fuel cells (DMFCs) have attracted extensive research for its high volumetric energy density and suitablity for portable applications, on top of that, mathonal is also a kind of abundant and environment-friendly resource[1]. Nevertheless, there are several barriers that restrain the extensive commercial applications of DMFCs, i.e. heat and water management, methanol crossover through the polymer proton exchange membrane, the slow kinetic reaction of methanol, durability and stability problem of the catalysts[2]. Specifically, the intermediate CO produced during the anodic process can heavily poison the surface of Pt catalyst and slow down the kinetic reaction of methanol. As a response, the most efficient method is to utilize Pt-based alloys[3, 4], such as Ru[5-9], Ni[10], Co[11] and Sn[12] which were chosen for their oxophilicity. The additional metals can easily adsorb oxygen species such as OH_{ad}, which can facilitate the transformation of CO to CO_2 through a known bi-functional mechanism[13]. While such a multi-component metallic electrocatalyst system has several drawbacks: quite tedious to achieve the uniform nanostructurization, impractical for commercial utilization, prone to segregation during device operation[14].

In addition, another effective strategy is to use metal oxides as Pt catalysts support, which can significantly enhance both the activity and stability of the catalysts[15]. Nowadays, many metal oxides such as WO_3[16], SnO_2[17], TiO_2[18, 19] and MoO_3[20, 21] have also attracted many attentions. In particular, ceria (cerium oxide) is more efficient for alleviating gaseous CO poisoning because of the particular fluorite

structure providing high surface area and the properties of variable valence states (redox Ce^{3+}/Ce^{4+} sites) increasing the oxygen storage capacity[14]. What's more, the interaction between CeO_2 and Pt can enhance the electrochemical activity by promoting the dispersion of Pt nanoparticles, and allow the OH_{ads} species to interact with CO on the surface of Pt. It is reported that the boundaries between Pt and CeO_x are all the active sites for ORR. Therefore, with the addition of CeO_2， the Pt/CeO_2 catalytic system can not only enhance the electrochemical activity of methanol oxidation, but also alleviate the CO poisoning issue[22].

Some literatures have reported the better performance of Pt with ceria based catalysts for methanol oxidation. According to Yu et al[23], the Pt/CeO_2-graphene catalysts also exhibited better methanol electrochemical oxidation than that of the Pt/graphene catalyst due to the addition of CeO_2. The detailed methanol oxidation catalysis performance data of these previous studies has been attached in Table 3. On the top of that, different CeO_2 content level also affects the ORR catalysis. Xu et al.[24] reported that with the introducing of CeO_2, $Pt/CeO_2/C$ have more oxygen atoms, and the percentage of surface oxygen on Pt NPs was increased from 59.65% of Pt/C to 69.19% of $Pt/20CeO_2/C$ containing 20wt% CeO_2, and even to 77.75% of $Pt/40CeO_2/C$ containing 40wt% CeO_2. The extremely enhanced oxygen spillover from CeO_2 to Pt surface should help increase the ORR activity. From the XPS analysis, the Ce-3d peaks of $Pt/CeO_2/C$ all showed a slightly negative shift when comparing with the pristine CeO_2, which is also a strong evidence of the interaction between Pt and Ce. But, the more CeO_2 content level inevitably leads to a rather low Pt^0

proportion and heavy aggregation, which reduces the active sites available. The strong interaction between Pt and Ce can help provide more oxygen atoms on the surface of Pt, but the preparation method, the CeO_2 content level, the ratio of Ce^{3+} and many other conditions may change the structure of Pt/CeOx system, which in turn affects the catalytic activity.

Until now, although many studies have investigated the effects of CeO_2 composition on the Pt/CeO_2-C catalysts[25-27], few studies have discussed the influence of CeO_2 pre-calcined temperatures on the methanol oxidation performance. Herein, Pt/CeO_2-C catalysts with CeO_2 pre-calcined at 300~600°C were investigated by the combination of hydrothermal calcination[28] and wet impregnation method[29] to explore the optimal pre-calcination temperature of CeO_2 in methanol electrooxidation. Electrocatalytic activity and stability of as-synthesized catalysts for MOR were characterized by cyclic voltammetry (CV), and amperometric i-t curve. According to this study's electrochemical results, Pt/CeO_2-C catalyst with CeO_2 pre-calcined at 400°C exhibit the superior CO tolerance performance for methanol electrochemical oxidation than that of the commercial Pt/C catalysts. The Pt/CeO_2-C catalyst with pre-calcined CeO_2 at 400°C has displayed the highest *ECSA* values at 68.14 $m^2\ g^{-1}_{Pt}$ and I_f/I_b ratio at 1.26, which are far larger than that of the commercial Pt/C catalyst at 53.23 $m^2\ g^{-1}_{Pt}$ and 0.79 respectively, implying the greatly enhanced CO tolerance performance.

2. Experimental

2.1 Preparation of Pt/CeO_2-C nanocatalysts

(1) Synthesis of CeO_2/C precursor

For a typical synthesis method, 0.051 g $Ce(NO_3)_3 \cdot 6H_2O$ and 0.1896 g carbon substrate (Vulcan XC-72R) were weighted and dissolved in 40 mL distilled water, and then the mixture was ultrasonicated for 30 min, continuously stirred for another 3 h, followed by dropping a certain concentration of ammonia into the mixed solution to create an alkaline environment. After the full reaction, the mixture was filtered for 3-5 times. The obtained material was dried at 80°C for 12 h. Then, the dried material was calcined in a saturated nitrogen atmosphere at different high temperature (300°C, 400°C, 500°C, 600°C) for 2 h, to obtain a homogeneous precursor CeO_2/C.

(2) Synthesis of Pt/CeO_2-C catalyst

The CeO_2/C precursor previously prepared was dispersed in distilled water with another 30 min's pre-ultrasonicating, followed by dropping a certain amount of H_2PtCl_6 solution with continuous stirring for 1 h, and then place the mixture into the oven until completely dry. Finally, the final product Pt/CeO_2-C catalyst was obtained after the reduction under 5% H_2/Ar at 300°C for 2 h. The obtained Pt/CeO_2-C samples at different pre-calcination temperatures of CeO_2 are marked as PC300, PC400, PC500 and PC600, respectively.

(3) Preparation of working electrode

To fabricate the working electrode, 10 mg catalysts in a 5 ml isopropanol and 100 μl Nafion (DE1020, 10wt%, DuPont) solution (0.05wt% Nafion dissolved in isopropanol) were mixed firstly, and ultrasonicated the mixture for 30 min to obtain a

homogeneous catalyst ink. Secondly, pip a total of 8-12 μL catalyst ink onto the glassy carbon substrate with a micropipette, yielding the Pt loading of 20 μg cm^{-2}. Beyond that, the glass carbon working electrode should be polished with 50 nm alumina powder, followed by being ultrasonicated with ultrapure water and ethanol for several times before all electrochemical measurements.

2.2 Characterization of physical properties

The X-ray diffraction (XRD) patterns were obtained with a Rigaku D/max 2550/PC diffractometer, operating with graphite-monochromatized Cu Kα radiation (λ = 1.54060 Å) ,and scans were done for 2θ ranging from 10° to 80°. The micro-structure of the catalysts was analyzed by transmission electron microscopy (TEM), model JEM-2100. The chemical composition was analyzed by inductively coupled plasma-atomic emission spectroscopy (ICP-AES, iCAP 6000 Radial, THERMO). The surface electron structure of Pt-CeO_2/C was analyzed by X-ray photoelectron spectrometer (XPS) with a Thermo ESCALab250 using monochromatized Al Ka radiation.

2.3 Electrochemical characterization

All the measurements were carried out in a conventional three-electrode cell at room temperature with a CHI 660D electrochemical analyzer (Chen Hua Instruments, Shanghai, China): the glassy carbon coated with the catalysts' ink as the working electrode, a platinum foil of 1 cm^2 as the counter electrode, and a saturated calomel electrode as the reference electrode, respectively. What needs to be explained is that all the potentials were converted to reversible hydrogen electrode (RHE) after the measurements.

The cyclic voltammetry (CV) tests were performed in a N_2-purged 0.5 M H_2SO_4 solution at room temperature. The potential was scanned in the range from 0 to 1.2 V (vs. RHE) at a scan rate of 50 mV s^{-1} for 40 cycles. The electrochemical surface area (ECSA) of each catalyst was calculated by the basis of the charges associated with the adsorption peak of hydrogen after double-layer correction at the positive scanning, and the calculation equation can be seen as follows[30-32]:

$$ECSA = \frac{Q_H}{210 \times W_{Pt}} \quad (1)$$

Where Q_H is calculated by the total charge (μC) of hydrogen adsorption peak area, W_{Pt} is the loading ($\mu C \cdot cm_{Pt}^{-2}$) of Pt on the working electrode, and the constant "210" represents the the charge needed to oxidize a monolayer of hydrogen on a bright Pt surface.

3. Results and discussion

3.1 Structure and composition analysis

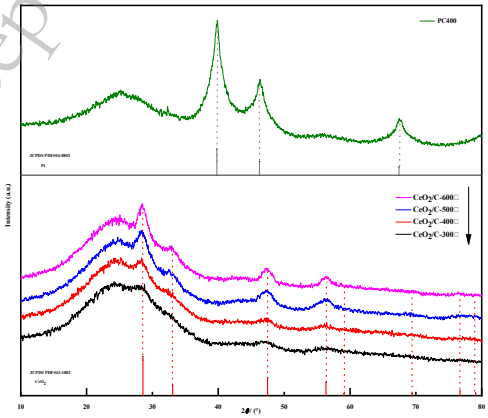

Fig. 1. XRD patterns of PC400 and CeO_2/C pre-calcined at different temperatures. The

standard patterns of CeO_2 (JCPDS PDF#43-1002) and Pt (JCPDS PDF#04-0802) are attached for comparison.

Fig. 1 shows the XRD patterns of PC400 catalyst and the precursor CeO_2/C pre-calcined at different temperature (300°C, 400°C, 500°C and 600°C, respectively). Firstly, the diffraction peaks at 2θ=39.85°, 46.30° and 67.50° can be clearly found in the PC400 sample, which can be indexed as the (111), (200) and (220) planes of the Pt face centered cubic crystalline (fcc) structure, respectively, while the diffraction peaks that belong to CeO_2 cannot be recognized in the PC400 sample. On the other hand, for the precursors' patterns, those diffraction peaks located at 28.21°, 32.92°, 47.24° and 56.20°, are ascribed to the (111), (200), (220) and (311) planes of the CeO_2 cubic fluorite structure[33, 34], respectively. Interestingly, the peak intensity of these facets increases with the rise of pre-calcination temperature. It should be noted that the disappeared CeO_2 diffraction peaks in PC400 sample may be assigned to the rather stronger Pt diffraction peaks hiding the CeO_2 diffraction peaks. It is reported that, the amorphous cerium oxide layer on Pt can prevent the Pt surface from oxidation, and in turn enhance the activity of the catalysts[35]. In addition, another diffraction peak can be observed at 25.3°, which belongs to the (002) plane of carbon.

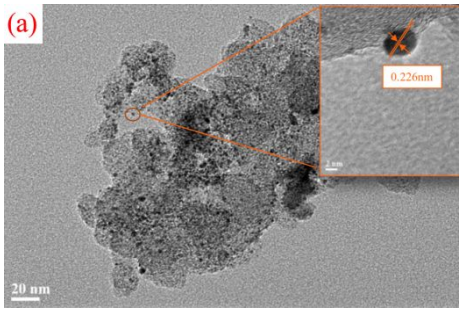

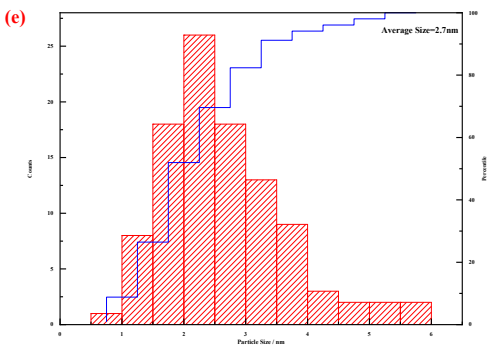

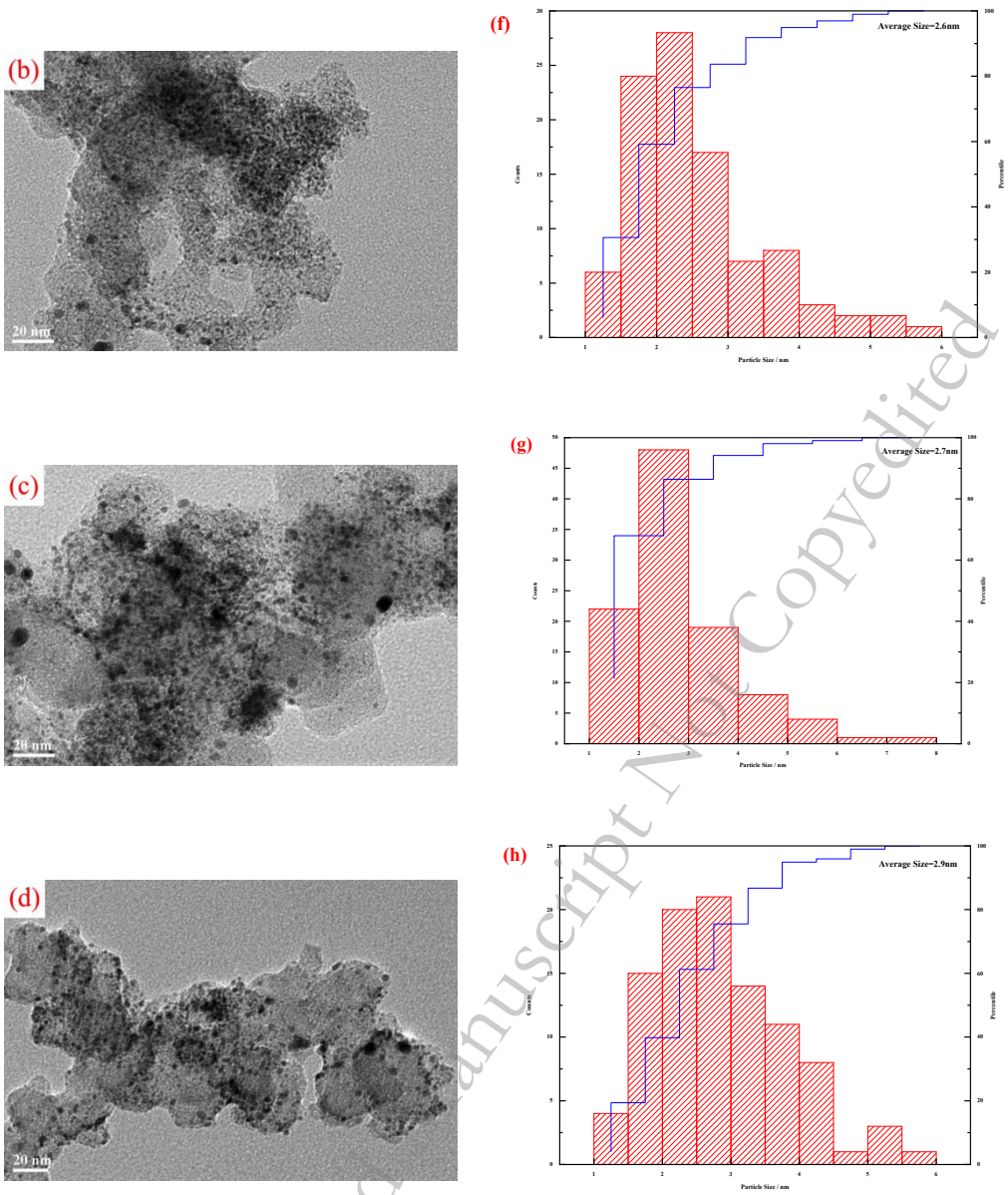

Fig. 2. TEM images (a~d) and average particle size distribution histograms (e~h) of Pt/CeO_2-C catalysts: PC300, PC400, PC500, PC600; HRTEM images of (a) PC300 is also attached.

Fig. 2 shows the TEM results of the as-synthesized Pt/CeO_2-C catalysts pre-calcined at different temperature. In general, all the four different catalysts show comparatively small sizes, calculated at about 2.7, 2.6 2.7 and 2.9 nm, respectively. However, the higher pre-calcination temperature (>400°C) leads to the agglomeration

of CeO_2 and the uneven distribution of the Pt nanoparticles. An interplanar spacing distance of 0.226 nm can be easily found in PC300, which is attributed to the Pt (111) plane[30, 32]. Furthermore, from the element mapping images of Ce, O and Pt in Fig. 3, we can see that the three elements of Ce, O and Pt in PC400 are evenly distributed on the surface of the carbon support. It is worth noting that the rather small loading amount of ceria can be explained for the reason why we cannot see the CeO_2 diffraction peak of PC400 in the XRD result.

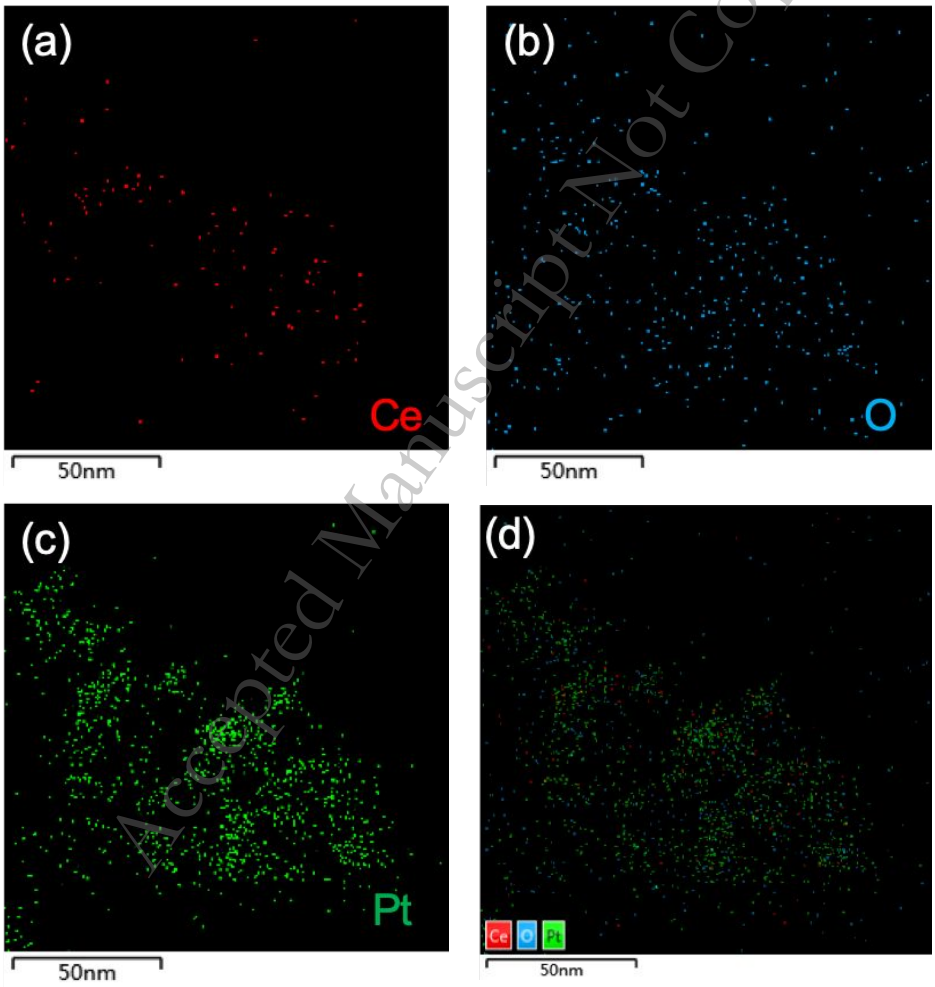

Fig. 3. TEM images of elemental mapping of (a) Ce, (b) O, (c) Pt and the (d) overlap.

Fig. 4 exhibits the Pt 4f and Ce 3d XPS peaks from PC400 sample, and the details of the fitting parameters' results were concluded in Table 1. Firstly, as for Pt 4f, the

peaks M and M' situated at 71.62 eV and 74.94 eV are ascribed to Pt(0), while the peaks N and N' situated at 72.88 eV and 76.33 eV belong to Pt^{2+}. It is obvious that Pt(0) is the main species in PC400 sample, accounting for 68.1% of total. However, compared to pure bulk Pt (70.9 eV), the binding energy shows a slight positive offset of 0.72 eV[31, 36] , which can be attributed to the strong interaction between Pt and CeO_2 in PC400 sample, resulting in a change in the electronic structure of the Pt metal[37, 38].

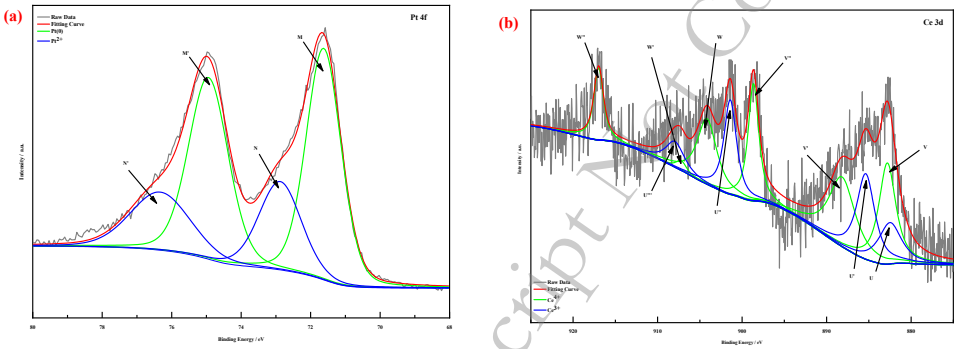

Fig. 4. XPS spectra for (a) Pt 4f, (b)Ce 3d of PC400 sample.

With regard to Ce 3d, the U series peaks at 882.51 eV, 885.36 eV, 901.40 eV and 907.94 eV are ascribed to Ce^{3+}, while the other six peaks at 882.81 eV, 888.16 eV, 898.65 eV, 904.15 eV, 907.21 eV and 916.98 eV belong to Ce^{4+}[39]. The total percentage composition of Ce^{4+} is predominant, accounting for 62.2% while that of Ce^{3+} is merely 37.8%. Just as we have discussed previously, the variable valence states (redox Ce^{3+}/Ce^{4+} sites) can greatly enhance the oxygen storage capacity, the oxygen vacancy in the Ce-O is a major advantage of the material. According to Yuan et al.[40], CeO_{2-x} with a higher concentration of oxygen vacancies has shown good ORR activity, excellent stability and good resistance to methanol crossover effects, therefore

benefiting the catalysis process of MOR.

Table 1. Binding energies and surface compositions from deconvolution of XPS spectra for PC400

Peak	Species		Binding energy (eV)	Relative ratio (%)	
Pt 4f	Pt (0)	M	71.62	35.90	68.1
		M'	74.94	32.20	
	Pt^{2+}	N	72.88	16.50	31.9
		N'	76.33	15.40	
Ce 3d	Ce^{4+}	V	882.81	15.42	62.2
		V'	888.16	16.45	
		V''	898.65	11.42	
		W	904.15	11.61	
		W'	907.21	0.94	
		W''	916.98	6.36	
	Ce^{3+}	U	882.51	8.54	37.8
		U'	885.36	14.08	
		U''	901.40	10.81	
		U'''	907.94	4.37	

3.2 MOR activity

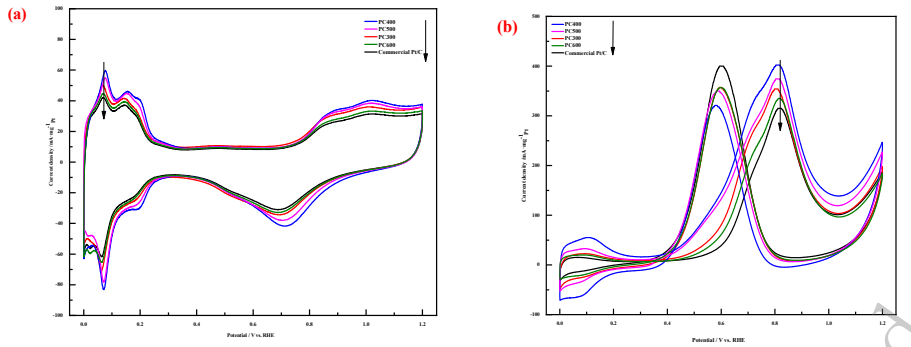

Fig. 5. Electrochemical data for the as-synthesized catalysts PC300, PC400, PC500, PC600 and the commercial Pt/C (JM, 20wt%): (a) CVs record in 0.5 M H_2SO_4 solution at a scan rate of 50 mV/s; (b) CVs record in 1 M CH_3OH and 0.5 M H_2SO_4 solution at a scan rate of 50 mV/s.

Fig. 5(a) shows the CV curves of the various catalysts measured at room temperature in a N_2-purged 0.5 M H_2SO_4 solution. The *ECSA* values of the as-synthesized catalysts PC300, PC400, PC500 and PC600 are calculated at 59.87, 68.14, 62.07 and 55.98 $m^2\ g^{-1}_{Pt}$, which are 1.12, 1.28, 1.16 and 1.05 times than that of the commercial Pt/C catalyst at 53.23 $m^2\ g^{-1}_{Pt}$, respectively. The electrochemical surface areas (*ECSAs*) of each catalyst was calculated by the basis of the charges associated with the absorption peak of hydrogen after double-layer correction with a reference value of 210 μC cm^{-2} for the hydrogen monolayer adsorption on Pt surface[41].From the *ECSA* analysis, we can easily conclude that the addition of CeO_2 can facilitate the electrochemical performance, and the optimal pre-calcination temperature is 400°C. The reason why the *ECSA* values of PC300~600 catalysts are larger than the commercial Pt/C catalyst may be that the addition of CeO_2 can enhance the distribution of Pt nanoparticles, which agrees with the TEM images' results.

A series of electrochemical tests of the as-prepared Pt/CeO_2-C catalysts towards

the methanol oxidation were executed by cyclic voltammograms (CVs) measurement. As can be seen from Fig. 5(b) and Table 2, the onsets potential of PC300, PC600 and the commercial Pt/C starts at 0.376 V, 0.380 V and 0.383 V, respectively, which are close to each other, however the onset potentials of PC400 and PC500 begin at 0.327 V and 0.33 V, respectively. On top of that, a method is used to compare the ratio of the forward scanning peak current density (I_f) and the backward scanning peak current density (I_b), which can represent the oxidation of methanol electrooxidation and the subsequent oxidation of the reactive carbonaceous species obtained from the positive potential scanning respectively[42, 43]. The ratio I_f/I_b can be used to reflect the catalysts' tolerance of CO poisoning[44]. As can be seen from Fig. 5(b), the ratio I_f/I_b of PC400 is highest among all the five catalysts, including the commercial Pt/C catalyst.what's more, with the increase of pre-calcination temperature of CeO_2 (>400°C), the ratio I_f/I_b shows a decrease trend, which can be explained by the poor dispersion of the nanocatalysts directly results in the terrible performance in both catalysis and CO poisoning tolerance[45]. Compared with the previous studies of Pt/CeO_2-C (Graphene) systems, our results' show CeO_2 pre-calcination temperature of Pt/CeO_2-C catalyst has an important effects on the CO tolerance performance of methanol oxidation. The detailed information can be found in Table 3.

Table 2. Comparison of electrocatalytic properties between the commercial and as-prepared catalysts

Catalysts	On-set potential (V vs. RHE)	I_f (mA mg^{-1}_{Pt})	I_f/I_b

PC300	0.376	354	0.99
PC400	0.327	405	1.26
PC500	0.33	376	1.07
PC600	0.380	335	0.92
Commercial Pt/C	0.383	316	0.79

Table 3. Comparison of electrocatalytic properties of I_f/I_b with previous Pt-CeO_2 studies

Number	Catalyst	I_f/I_b	Reference
1	Pt/CeO_2-Graphene	<1	[46]
2	Pt/3wt%CeO_2-C	0.55	[47]
3	Pt/6wt%CeO_2-C	0.53	[47]
4	Pt/9wt%CeO_2-C	1.45	[47]
5	Pt/12wt%CeO_2-C	1.23	[47]
6	Pt–3%CeO_2/Graphene	1.41	[48]
7	Pt–5%CeO_2/Graphene	1.45	[48]
8	Pt–7%CeO_2/Graphene	1.48	[48]
9	Pt–10%CeO_2/Graphene	1.35	[48]
10	PC300	0.99	This work
11	PC400	1.26	This work
12	PC500	1.07	This work
13	PC600	0.92	This work

*I_f–current density associated with anodic peak in forward scan;

*I_b–current density associated with anodic peak in backward scan.

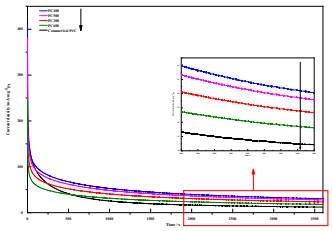

Fig. 6. Amperometric i-t curves collected for 1 h at 0.6 V (vs. RHE) for the catalysts in a 1 M CH_3OH and 0.5 M H_2SO_4 solution at room temperature.

The chronoamperometric technique is an effective method to evaluate the catalysts' electrocatalytic activity and stability. It is obvious that PC400 displays the highest current density and the smallest current decay among all the other catalysts, including the commercial Pt/C. Specifically, the current density values of PC300, PC400, PC500, PC600 and the commercial Pt/C after 3600 s constant potential electrolysis at 0.6 V (vs. RHE) in the amperometric i-t curves are 23.4, 28.0, 19.4, 18.1 and 12.2 mA mg^{-1}_{Pt}, respectively, indicating that PC400 possesses relatively highest electrocatalytic activity and strongest tolerance to carbonaceous by-products produced during the methanol oxidation.

The enhanced catalysis activity and stability of the as-synthesized PC300~600 catalysts in methanol oxidation reaction can be explained as follows:

Firstly, Ce 3d orbitals can change the electronic structure of Pt, and weaken the adsorption of CO-based carbonaceous by-products on the surface of Pt, CO can also be oxidized by CeO_2 on the surface of Pt at the same time[49, 50]. As a result, the reduction of carbon-containing intermediates adsorbed on the platinum surface can effectively

improve the electrocatalytic activity of methanol oxidation[26].

Secondly, CeO_2 can both improve the distribution of Pt nanoparticles[51] and provide the OH_{ad} species for electro-oxidation to interact with the carbonaceous intermediates adsorbed by the catalysts, and then generate CO_2 during methanol oxidation, which is a bi-functional mechanism, just as the following formulas explaining[52-55]:

$$CeO_2 + H_2O \rightarrow CeO_2\text{-}OH_{ad} + H^+ + e^- \quad (1)$$

$$Pt\text{-}CO_{ad} + CeO_2\text{-}OH_{ad} \rightarrow Pt + CeO_2 + CO_2 + H^+ + e^- \quad (2)$$

$$Pt\text{-}CeO_2 + xCO \rightarrow Pt\text{-}CeO_{2-x} + xCO_2 \quad (3)$$

Lastly, the optimum pre-calcination temperature (400°C) may contribute to the generation of the CeO_2 with fluorite structure and promote the interaction among CeO_2, Pt and carbon support. While the higher temperature (>400°C) may lead to the agglomeration of CeO_2, which will negatively impact the homogenous distribution of Pt nanoparticles[32, 56].

4. Conclusions

In this paper, Pt/CeO_2-C catalysts were successfully prepared, electrocatalysis performance was also tested in acidic medium to investigate the effect of CeO_2 pre-calcined at different temperature (300~600°C) on the performance of Pt/CeO_2-C electrocatalysts for methanol oxidation. PC400 exhibited the best methanol electro-oxidation among all catalysts. Specifically, The *ECSA* of PC400 is 53.33 $m^2\ g^{-1}_{Pt}$, which is 1.28 times than that of the commercial Pt/C catalyst, and the ratio I_f/I_b of

PC400 is 1.26, which is 1.59 times than that of the commercial Pt/C catalyst. Furthermore, amperometric i-t curves and continued voltammogram cycles of PC400 displayed an excellent stability performance compared with other catalysts as well. In conclusion, introducing CeO_2 from a proper pre-calcination temperature(～400°C) can promote the dispersion of Pt nanoparticles with a rather small size (～2.7 nm) and provide a higher tolerance to carbonaceous species produced during the methanol oxidation, which directly enhances the performances of catalysis activity and stability.

5 Acknowledgments

This work was financially supported by National Natural Science Foundation of China (No. 51774145).

References

[1] H. Xu, A.L. Wang, Y.X. Tong, and G.R. Li, Enhanced Catalytic Activity and Stability of Pt/CeO_2/PANI Hybrid Hollow Nanorod Arrays for Methanol Electro-oxidation, *ACS Catal.*, 6(2016), No. 8, p. 5198.

[2] S.S. Munjewar, S.B. Thombre, and R.K. Mallick, Approaches to overcome the barrier issues of passive direct methanol fuel cell - Review, *Renewable Sustainable Energy Rev.*, 67(2017), p. 1087.

[3] J.M. Léger, S. Rousseau, C. Coutanceau, F. Hahn, and C. Lamy, How bimetallic electrocatalysts does work for reactions involved in fuel cells?, *Electrochim. Acta*, 50(2005), No. 25-26, p. 5118.

[4] N.S. Pai, P.S. Chang, and S.K. Yen, Platinum/vivianite bifunction catalysts for DMFC, *Int. J. Hydrogen Energy*, 38(2013), No. 13, p. 5259.

[5] C. Jackson, O. Conrad, and P. Levecque, Systematic Study of Pt-Ru/C Catalysts Prepared by Chemical Deposition for Direct Methanol Fuel Cells, *Electrocatalysis*, 8(2017), No. 3, p. 224.

[6] A. Dickinson, L. Carrette, J. Collins, K. Friedrich, and U. Stimming, Preparation of a Pt-Ru/C catalyst from carbonyl complexes for fuel cell applications, *Electrochim. Acta*, 47(2002), No. 22-23, p. 3733.

[7] V. Thiagarajan, P. Karthikeyan, R. Manoharan, S. Sampath, A. Hernández-Ramírez, M. Sánchez-Castro, I. Alonso-Lemus, and F. Rodríguez-Varela, Pt-Ru-$NiTiO_3$ Nanoparticles Dispersed on Vulcan as High Performance Electrocatalysts for the Methanol Oxidation Reaction (MOR), *Electrocatalysis*, 9(2018), No. 5, p. 582.

[8] D. Pan, X. Li, and A. Zhang, Platinum assisted by carbon quantum dots for methanol electro-oxidation, *Appl. Surf. Sci.*, 427(2018), p. 715.

[9] H. Liu, C. Song, L. Zhang, J. Zhang, H. Wang, and D.P. Wilkinson, A review of anode catalysis in the direct methanol fuel cell, *J. Power Sources*, 155(2006), No. 2, p. 95.

[10] A. Glüsen, F. Dionigi, P. Paciok, M. Heggen, M. Müller, L. Gan, P. Strasser, R.E. Dunin-Borkowski, and D. Stolten, Dealloyed PtNi-Core–Shell Nanocatalysts Enable Significant Lowering of Pt Electrode Content in Direct Methanol Fuel Cells, *ACS Catal.*, 9(2019), No. 5, p. 3764.

[11] A. Serra, M. Montiel, E. Gomez, and E. Valles, Electrochemical Synthesis of Mesoporous CoPt Nanowires for Methanol Oxidation, *Nanomaterials*, 4(2014), No. 2, p. 189.

[12] L.G. Martin, I. Green, X. Wang, S. Pasupathi, and B.G. Pollet, Pt–Sn/C as a Possible Methanol-Tolerant Cathode Catalyst for DMFC, *Electrocatalysis*, 4(2013), No. 3, p. 144.

[13] S. Zhang, Z. Xia, T. Ni, Z. Zhang, Y. Ma, and Y. Qu, Strong electronic metal-support interaction of Pt/CeO2 enables efficient and selective hydrogenation of quinolines at room temperature, *J. Catal.*, 359(2018), p. 101.

[14] S.K. Meher and G.R. Rao, Polymer-Assisted Hydrothermal Synthesis of Highly Reducible Shuttle-Shaped CeO_2: Microstructural Effect on Promoting Pt/C for Methanol Electrooxidation, *ACS Catal.*, 2(2012), No. 12, p. 2795.

[15] L. Nie, D.H. Mei, H.F. Xiong, B. Peng, Z.B. Ren, X.I.P. Hernandez, A. DeLariva, M. Wang, M.H. Engelhard, L. Kovarik, A.K. Datye, and Y. Wang, Activation of surface lattice oxygen in single-atom Pt/CeO_2 for low-temperature CO oxidation, *Science*, 358(2017), No. 6369, p. 1419.
[16] Z. Cui, L. Feng, C. Liu, and W. Xing, Pt nanoparticles supported on WO_3/C hybrid materials and their electrocatalytic activity for methanol electro-oxidation, *J. Power Sources*, 196(2011), No. 5, p. 2621.
[17] C.C. Winter, A new test for vesicoureteral reflux: an external technique using radioisotopes, *Trans West Sect Am Urol Assoc*, 25(1958), No. 4, p. 105.
[18] H. Lin, Y.B. Dong, and L.Y. Jiang, Preparation of calcium carbonate particles coated with titanium dioxide, *Int. J. Miner. Metall. Mater.*, 16(2009), No. 5, p. 592.
[19] T.T. Ai, F. Wang, and X.M. Feng, Oxidation behavior of in-situ Al_2O_3/TiAl composites at 900° C in static air, *Int. J. Miner. Metall. Mater.*, 16(2009), No. 3, p. 339.
[20] P. Justin and G. Ranga Rao, Methanol oxidation on MoO_3 promoted Pt/C electrocatalyst, *Int. J. Hydrogen Energy*, 36(2011), No. 10, p. 5875.
[21] X.Y. Wang, J.C. Zhang, X.D. Cao, Y.S. Jiang, and H. Zhu, Synthesis and characterization of Pt-MoO_x-TiO_2 electrodes for direct ethanol fuel cells, *Int. J. Miner. Metall. Mater.*, 18(2011), No. 5, p. 594.
[22] S. Song, X. Wang, and H. Zhang, CeO_2-encapsulated noble metal nanocatalysts: enhanced activity and stability for catalytic application, *NPG Asia Mater.*, 7(2015), No. 5, p. e179.
[23] S. Yu, Q. Liu, W. Yang, K. Han, Z. Wang, and H. Zhu, Graphene–CeO_2 hybrid support for Pt nanoparticles as potential electrocatalyst for direct methanol fuel cells, *Electrochim. Acta*, 94(2013), p. 245.
[24] F. Xu, D. Wang, B. Sa, Y. Yu, and S. Mu, One-pot synthesis of Pt/CeO_2/C catalyst for improving the ORR activity and durability of PEMFC, *Int. J. Hydrogen Energy*, 42(2017), No. 18, p. 13011.
[25] W. Wang, Y. Dong, Y. Yang, D. Chai, Y. Kang, and Z. Lei, CeO_2 overlapped with nitrogen-doped carbon layer anchoring Pt nanoparticles as an efficient electrocatalyst towards oxygen reduction reaction, *Int. J. Hydrogen Energy*, 43(2018), No. 27, p. 12119.
[26] H. Xu, A.L. Wang, Y.X. Tong, and G.R. Li, Enhanced Catalytic Activity and Stability of Pt/CeO2/PANI Hybrid Hollow Nanorod Arrays for Methanol Electro-oxidation, *ACS Catal.*, 6(2016), No. 8, p. 5198.
[27] G. L. Cordeiro, Improved Pt/CeO_2 Electrocatalysts for Ethanol Electro-oxidation, *Int. J. Electrochem. Sci.*(2018), p. 6388.
[28] B. He, Q. Zhao, Z. Zeng, X. Wang, and S. Han, Effect of hydrothermal reaction time and calcination temperature on properties of Au@CeO_2 core–shell catalyst for CO oxidation at low temperature, *J. Mater. Sci.*, 50(2015), No. 19, p. 6339.
[29] Z. Qi, C. Xiao, C. Liu, T.W. Goh, L. Zhou, R. Maligal-Ganesh, Y. Pei, X. Li, L.A. Curtiss, and W. Huang, Sub-4 nm PtZn Intermetallic Nanoparticles for Enhanced Mass and Specific Activities in Catalytic Electrooxidation Reaction, *J. Am. Chem. Soc.*, 139(2017), No. 13, p. 4762.
[30] J. Yang, X. Tan, Y. Qian, L. Li, Y. Xue, Z. Dai, H. Wang, W. Qu, and Y. Chu,

Methanol oxidation on Pt/CeO_2@C–N electrocatalysts prepared by the in-situ carbonization of polyvinylpyrrolidone, *J. Appl. Electrochem.*, 46(2016), No. 7, p. 779.
[31] D.M. Gu, Y.Y. Chu, Z.B. Wang, Z.Z. Jiang, G.P. Yin, and Y. Liu, Methanol oxidation on Pt/CeO_2–C electrocatalyst prepared by microwave-assisted ethylene glycol process, Appl. Catal., B, 102(2011), No. 1-2, p. 9.
[32] J. Yu and B. Wang, Effect of calcination temperature on morphology and photoelectrochemical properties of anodized titanium dioxide nanotube arrays, Appl. Catal., B, 94(2010), No. 3-4, p. 295.
[33] F. Abbas, J. Iqbal, T. Jan, N. Badshah, Q. Mansoor, and M. Ismail, Structural, morphological, Raman, optical, magnetic, and antibacterial characteristics of CeO_2 nanostructures, *Int. J. Miner. Metall. Mater.*, 23(2016), No. 1, p. 102.
[34] Z.Y. Cai, B. Song, L.F. Li, Z. Liu, and X.K. Cui, Effect of CeO_2 on heat transfer and crystallization behavior of rare earth alloy steel mold fluxes, *Int. J. Miner. Metall. Mater.*, 26(2019), No. 5, p. 565.
[35] K. Fugane, T. Mori, D.R. Ou, A. Suzuki, H. Yoshikawa, T. Masuda, K. Uosaki, Y. Yamashita, S. Ueda, K. Kobayashi, N. Okazaki, I. Matolinova, and V. Matolin, Activity of oxygen reduction reaction on small amount of amorphous CeO_x promoted Pt cathode for fuel cell application, *Electrochim. Acta*, 56(2011), No. 11, p. 3874.
[36] B. Kennedy and A. Hamnett, Oxide formation and reactivity for methanol oxidation on platinised carbon anodes, *J. Electroanal. Chem. Interfacial Electrochem.*, 283(1990), No. 1-2, p. 271.
[37] F.ç. Larachi, J. Pierre, A. Adnot, and A. Bernis, Ce 3d XPS study of composite $Ce_xMn_{1-x}O_{2-y}$ wet oxidation catalysts, *Appl. Surf. Sci.*, 195(2002), No. 1-4, p. 236.
[38] J. Zhao, W. Chen, Y. Zheng, and X. Li, Novel carbon supported hollow Pt nanospheres for methanol electrooxidation, *J. Power Sources*, 162(2006), No. 1, p. 168.
[39] A.B. Yousaf, M. Imran, N. Uwitonze, A. Zeb, S.J. Zaidi, T.M. Ansari, G. Yasmeen, and S. Manzoor, Enhanced electrocatalytic performance of Pt_3Pd_1 alloys supported on CeO_2/C for methanol oxidation and oxygen reduction reactions, *J. Phys. Chem. C*, 121(2017), No. 4, p. 2069.
[40] X. Yuan, H. Ge, X. Liu, X. Wang, W. Chen, W. Dong, and F. Huang, Efficient catalyst of defective CeO_{2-x} and few-layer carbon hybrid for oxygen reduction reaction, *J. Alloys Compd.*, 688(2016), p. 613.
[41] C. Wei, S. Sun, D. Mandler, X. Wang, S.Z. Qiao, and Z.J. Xu, Approaches for measuring the surface areas of metal oxide electrocatalysts for determining their intrinsic electrocatalytic activity, *Chem. Soc. Rev.*, 48(2019), No. 9, p. 2518.
[42] Y. Zhao, L. Zhan, J. Tian, S. Nie, and Z. Ning, Enhanced electrocatalytic oxidation of methanol on Pd/polypyrrole–graphene in alkaline medium, *Electrochim. Acta*, 56(2011), No. 5, p. 1967.
[43] C.C. Ting, C.H. Chao, C.Y. Tsai, I.K. Cheng, and F.M. Pan, Electrocatalytic performance of Pt nanoparticles sputter-deposited on indium tin oxide toward methanol oxidation reaction: The particle size effect, *Appl. Surf. Sci.*, 416(2017), p. 365.
[44] F. Zhan, T. Bian, W. Zhao, H. Zhang, M. Jin, and D. Yang, Facile synthesis of Pd–Pt alloy concave nanocubes with high-index facets as electrocatalysts for methanol oxidation, *CrystEngComm*, 16(2014), No. 12, p. 2411.

[45] G. Bai, C. Liu, Z. Gao, B. Lu, X. Tong, X. Guo, and N. Yang, Atomic Carbon Layers Supported Pt Nanoparticles for Minimized CO Poisoning and Maximized Methanol Oxidation, *Small*, 15(2019), No. 38, p. 1902951.
[46] H. Chen, J. Duan, X. Zhang, Y. Zhang, C. Guo, L. Nie, and X. Liu, One step synthesis of Pt/CeO_2-graphene catalyst by microwave-assisted ethylene glycol process for direct methanol fuel cell, *Mater. Lett.*, 126(2014), No., p. 9.
[47] M.A. Scibioh, S.K. Kim, E.A. Cho, T.H. Lim, S.A. Hong, and H.Y. Ha, Pt-CeO_2/C anode catalyst for direct methanol fuel cells, Appl. Catal., B, 84(2008), No. 3-4, p. 773.
[48] S. Yu, Q. Liu, W. Yang, K. Han, Z. Wang, and H. Zhu, Graphene-CeO_2 hybrid support for Pt nanoparticles as potential electrocatalyst for direct methanol fuel cells, *Electrochim. Acta*, 94(2013), No., p. 245.
[49] C.T. Campbell and C.H. Peden, Chemistry. Oxygen vacancies and catalysis on ceria surfaces, *Science*, 309(2005), No. 5735, p. 713.
[50] E. Mamontov, W. Dmowski, T. Egami, and C.C. Kao, Electronic excitation in a catalytic support oxide, CeO_2, *J. Phys. Chem. Solids*, 61(2000), No. 3, p. 431.
[51] H. Chen, J. Duan, X. Zhang, Y. Zhang, C. Guo, L. Nie, and X. Liu, One step synthesis of Pt/CeO_2–graphene catalyst by microwave-assisted ethylene glycol process for direct methanol fuel cell, *Mater. Lett.*, 126(2014), p. 9.
[52] K. Yoon, Y. Yang, P. Lu, D. Wan, H.C. Peng, K. Stamm Masias, P.T. Fanson, C.T. Campbell, and Y. Xia, A highly reactive and sinter-resistant catalytic system based on platinum nanoparticles embedded in the inner surfaces of CeO_2 hollow fibers, *Angew. Chem. Int. Ed. Engl.*, 51(2012), No. 38, p. 9543
[53] A. Kabbabi, R. Faure, R. Durand, B. Beden, F. Hahn, J.M. Leger, and C. Lamy, In situ FTIRS study of the electrocatalytic oxidation of carbon monoxide and methanol at platinum–ruthenium bulk alloy electrodes, *J. Electroanal. Chem.*, 444(1998), No. 1, p. 41.
[54] M.-S. Ekrami-Kakhki, N. Farzaneh, S. Abbasi, and B. Makiabadi, Electrocatalytic activity of Pt nanoparticles supported on novel functionalized reduced graphene oxide-chitosan for methanol electrooxidation, *J. Mater. Sci.: Materials in Electronics*, 28(2017), No. 17, p. 12373.
[55] S. Ramani, S. Sarkar, V. Vemuri, and S.C. Peter, Chemically designed CeO_2 nanoboxes boost the catalytic activity of Pt nanoparticles toward electro-oxidation of formic acid, *J. Mater. Chem. A*, 5(2017), No. 23, p. 11572.
[56] J. Yang, Y. Chu, L. Li, H. Wang, Z. Dai, and X.Y. Tan, Effects of calcination temperature and CeO_2 contents on the performance of Pt/CeO_2−CNTs hybrid nanotube catalysts for methanol oxidation, *J. Appl. Electrochem.*, 46(2016), No. 3, p. 369.